Supplemental figure 1

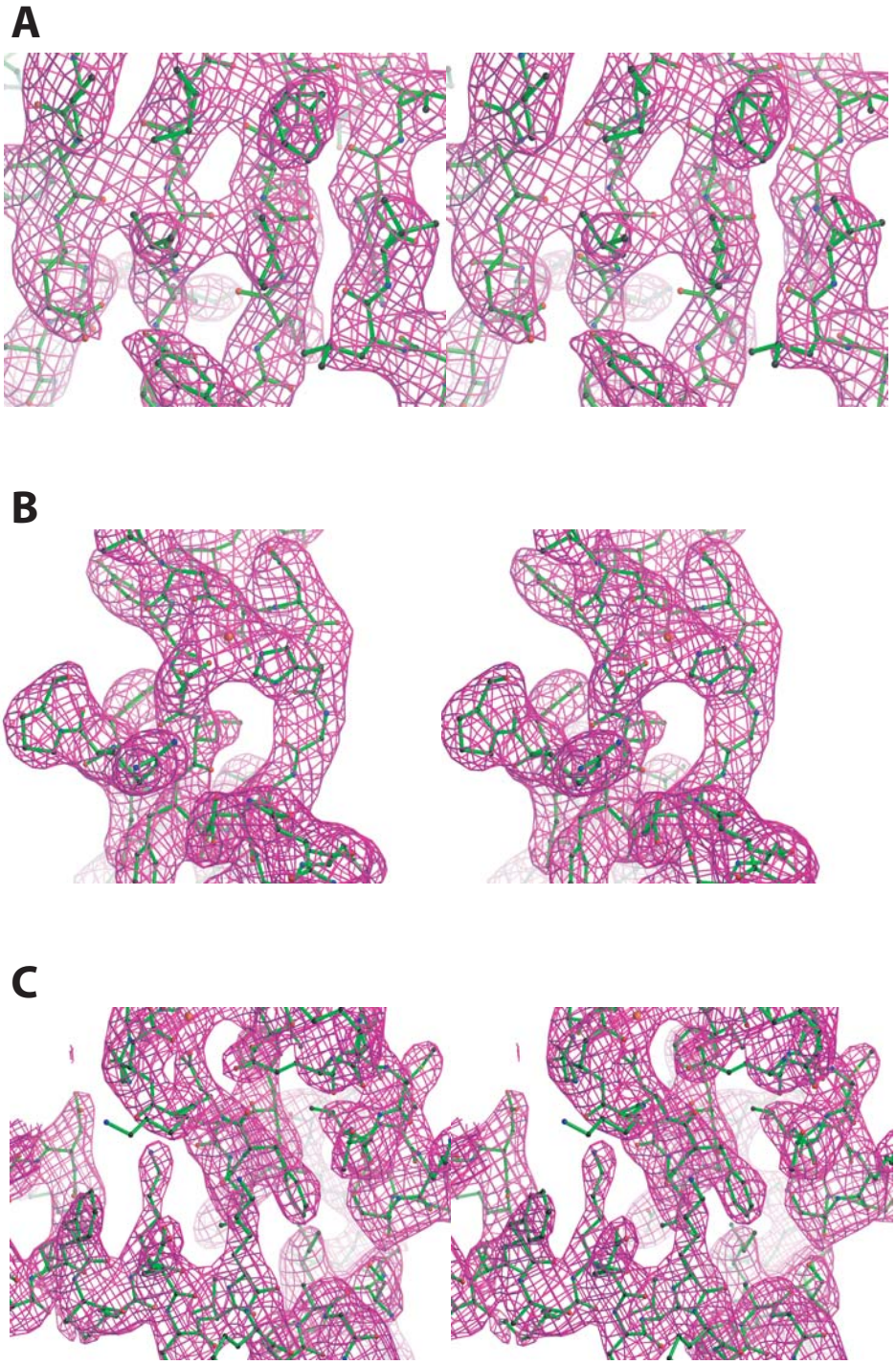

Stereoview of simulated annealing omit maps (contoured at 3.5 σ level) of EF-CaM complex. The representative maps (magenta) and structure models (green) of the PABD (A), active site (B) and interface between N-CaM and helical domain (C) are shown.

Supplemental Figure 2

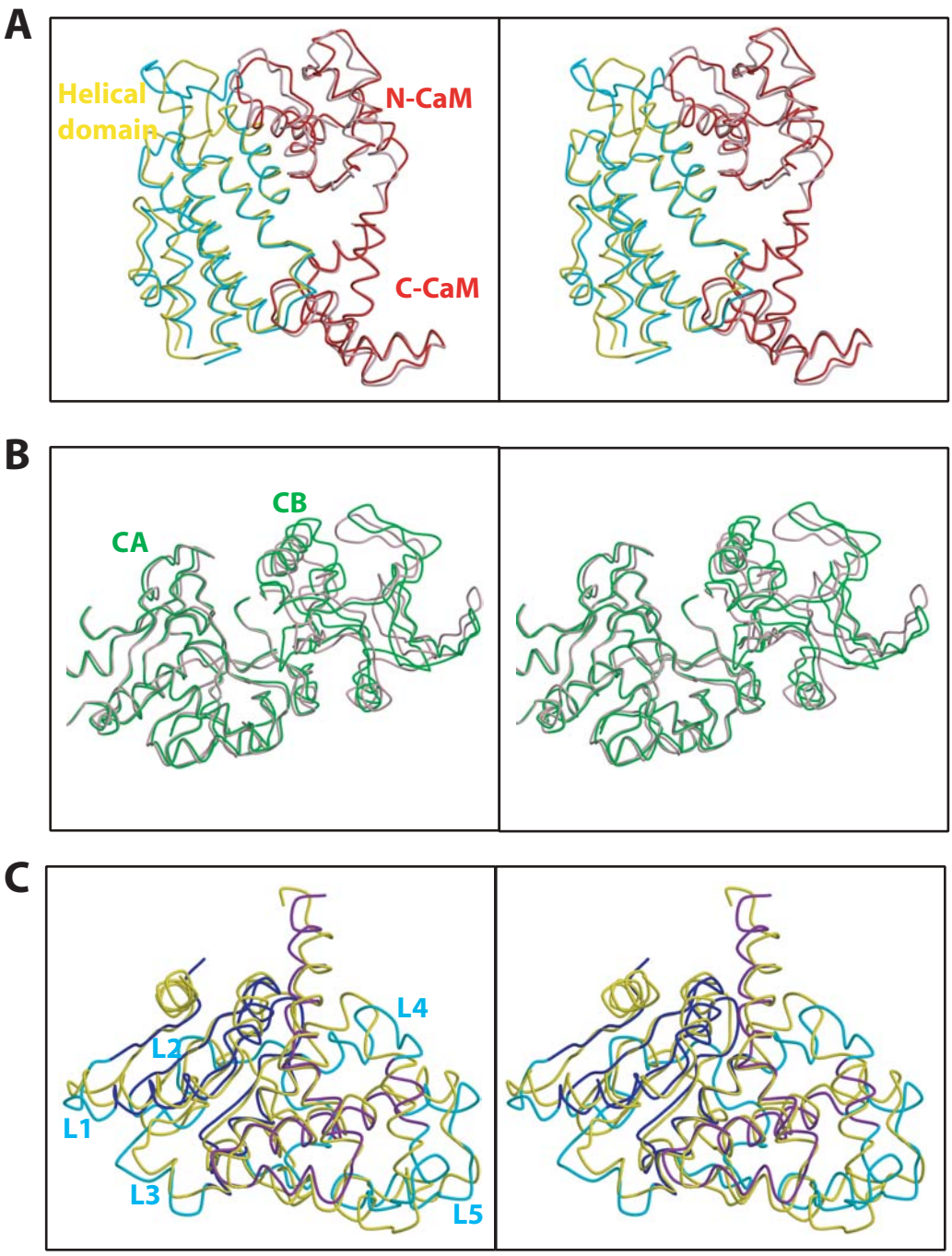

Stereoview of the comparison in EF-ACD-CaM and EF-CaM complex. (A) N-CaM and the helical domain. The helical domain and CaM in EF-CaM is colored yellow and red, respectively while those in EF-ACD-CaM are cyan and pink, respectively. (B) Domains CA and CB region. They are colored green in EF-CaM and pink in EF-ACD-CaM. CB region requires a rotation after the superimposition of CA domain. (C) PA binding domain. N-terminal domain and C-terminal domain of EF are colored blue and purple in EF-CaM complex. Loops L1-L5 are colored cyan and LF is colored yellow.

Supplemental Figure 3

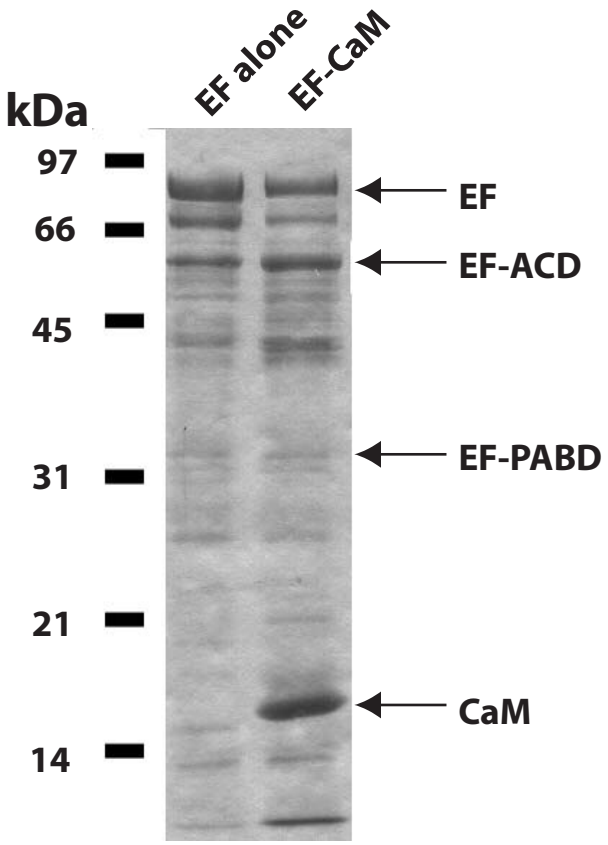

Tryptic digestion of EF alone and EF-CaM complex. 25 μg EF protein on ice was digested with 1.5 μg trypsin for 2 minutes in 50 μl reaction buffer (20 mM Tris-HCl [pH 8.6], 20 mM NaCl). In the EF-CaM complex, additional 11 μg CaM and 1 mM $CaCl_2$ were included.

Supplemental Figure 4

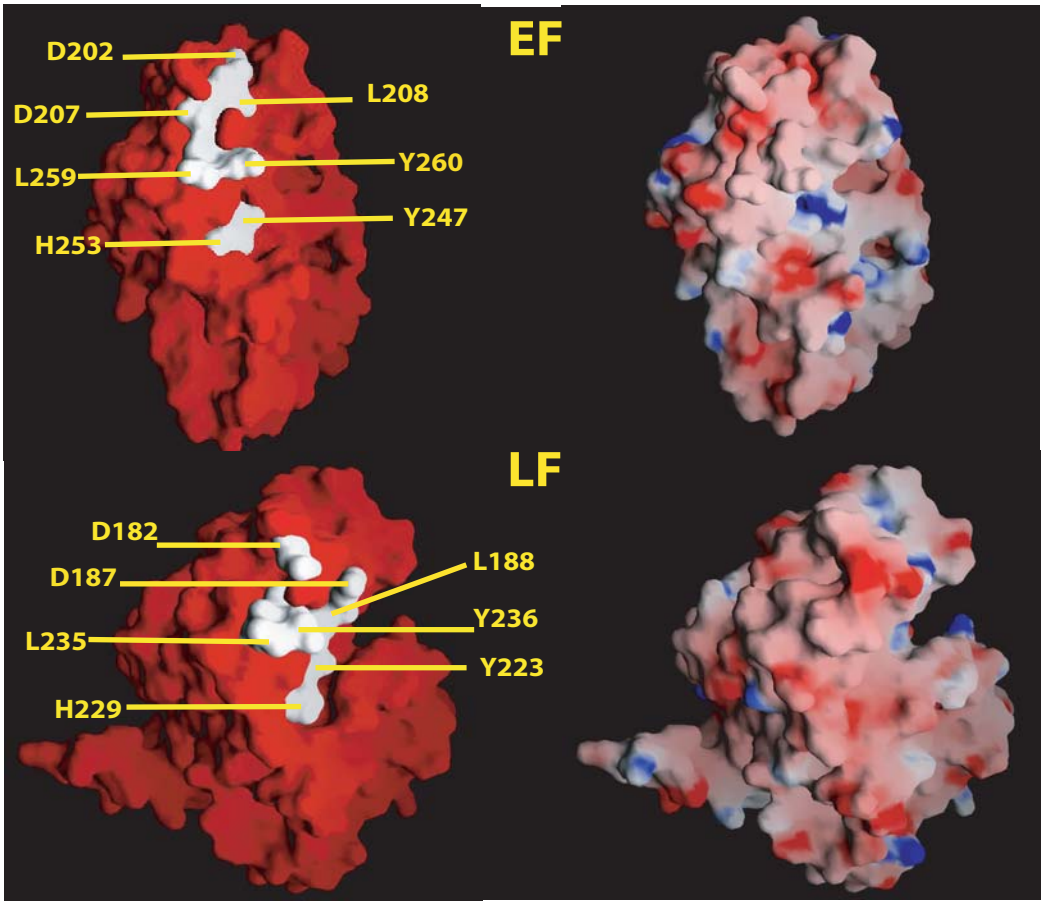

PA binding site of EF. Left, surface representation of EF and LF depicting the cluster of PA binding residues. Molecular surfaces of PA binding domains of EF and LF are in red and the residues that affect PA binding are in white (Lacy et al J Biol Chem 277: 3006, 2002). Right, electrostatic surface presentation (at the 10 KT e^{-1} level) of PA binding domains of EF and LF. GRASP program (Nicholls et al., Proteins 11:281, 1991) were used to calculate the surface potential. Negative surface is colored red, positive surface blue, and neutral surface white.

Supplemental Figure 5

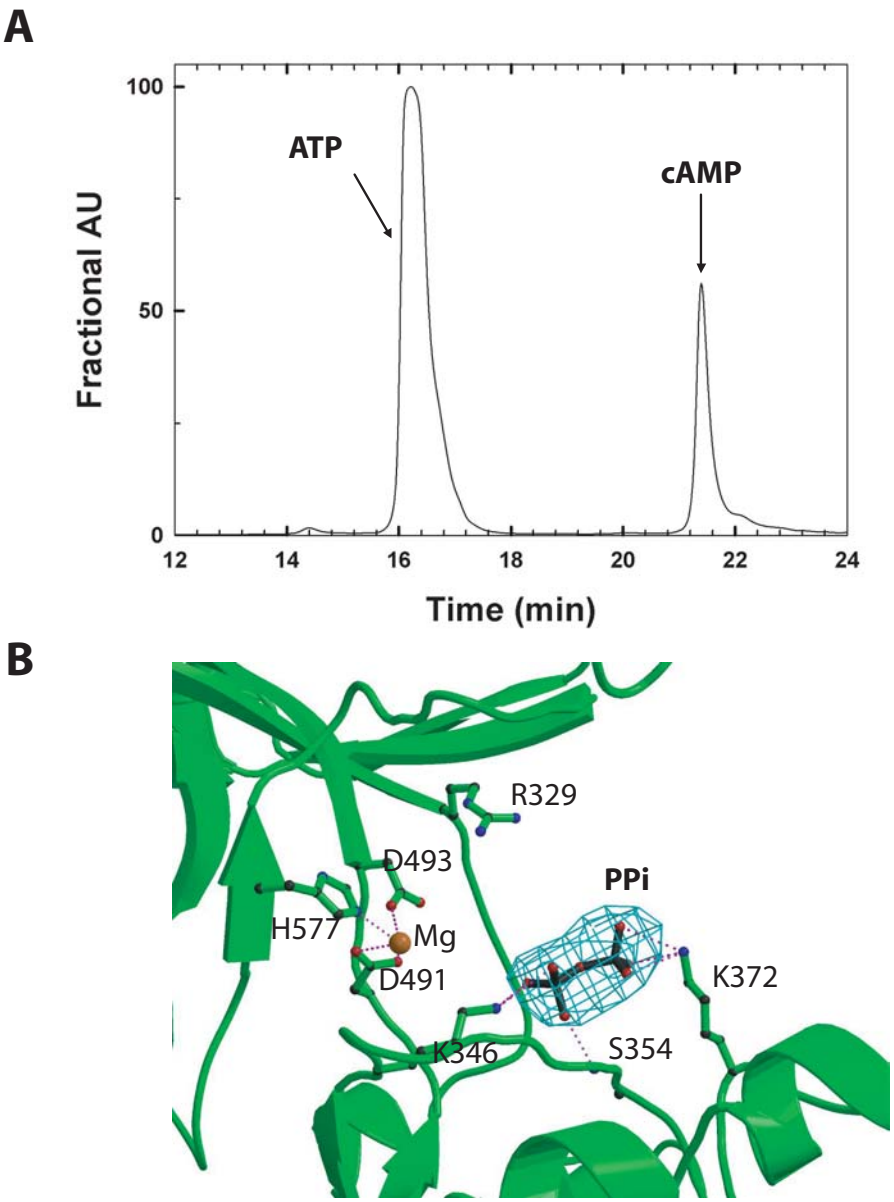

EF-CaM complex crystals are catalytically active. (A) HPLC elution profile of nucleotides after the incubation with EF-CaM crystals. Two EF-CaM crystals (~0.7mm X 0.3mm X 0.05mm) were washed with mother liquor of crystallization solution (28% PEG400, 0.2M $MgCl_2$, 0.1M Tris-HCl pH8.5) for three times to remove the loosely associated EF-CaM complex. These crystals were transfered into 200 μl mother liquor mixed with 5 mM ATP and kept at 4 ^{o}C for 30 minutes. The solution was then extracted by phenol and chloroform and analyzed by HPLC C18 column as described (Guo et al J Biol Chem 279:19427, 2004). Such experiment was repeated again using the same crystals. Under this condition, 21 +/- 0.5% ATP were converted to cAMP. (B) Active site of structure of EF-CaM that was soaked with Rp-ATPαS. The simulated annealing omit map was contoured at 4.0σ level. Oxygen, nitrogen, carbon and metal atoms are in red, blue, black and orange, respectively. Secondary structures of EF and pyrophosphate are in green and black, respectively. Rp-ATPαS is a gift from Fritz Eckstein and it is the same batch of nucleotide that has been used to obtain the structure of Rp-ATPαS bounded VC1-2C2-Gsα-forskolin complex (Tesmer et al Science 285:756, 1999). Mass spectroscopy reveals that this batch of Rp-ATPαS is greater than 95% pure and has no observable contamination of pyrophosphate.

Supplemental Figure 6

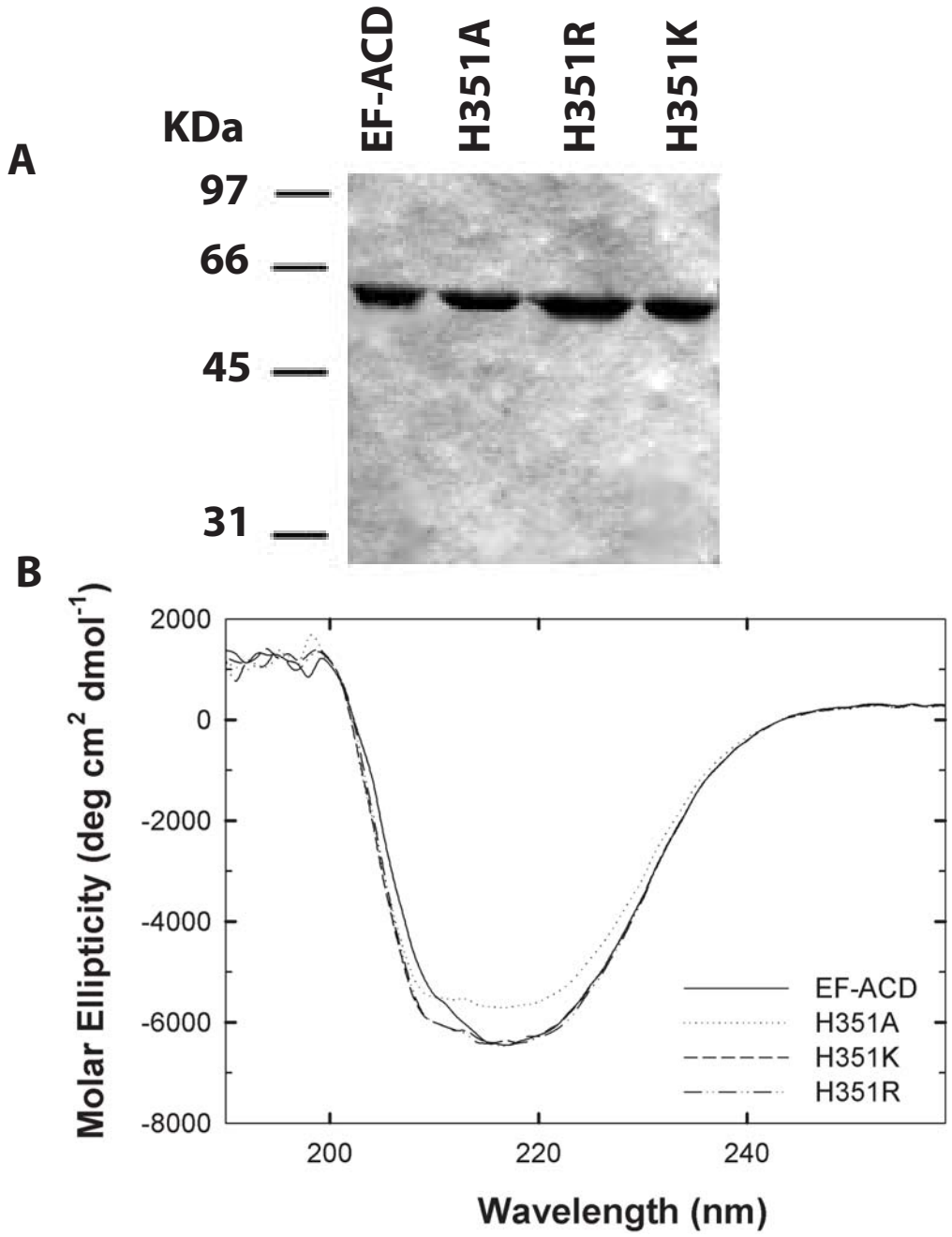

Characterization of H351 mutants of EF-ACD. (A) Coomassie blue staining of purified EF-ACD protein and its mutants on SDS-PAGE (2 μg each). (B) Circular Dichroism Spectroscopy of EF-ACD and its mutants. CD spectra (200-260 nm) were collected on Aviv 202 Circular Dichroism spectrophotometer using 0.1 cm path length cell and maintaining the temperature at 30 ^{o}C . The spectra were obtained in 10 mM phosphate buffer at pH 7.7 with the protein concentration of 1 μg/ml. Raw data were corrected for buffer contributions and converted to mean residue ellipticity.

Supplemental Figure 7

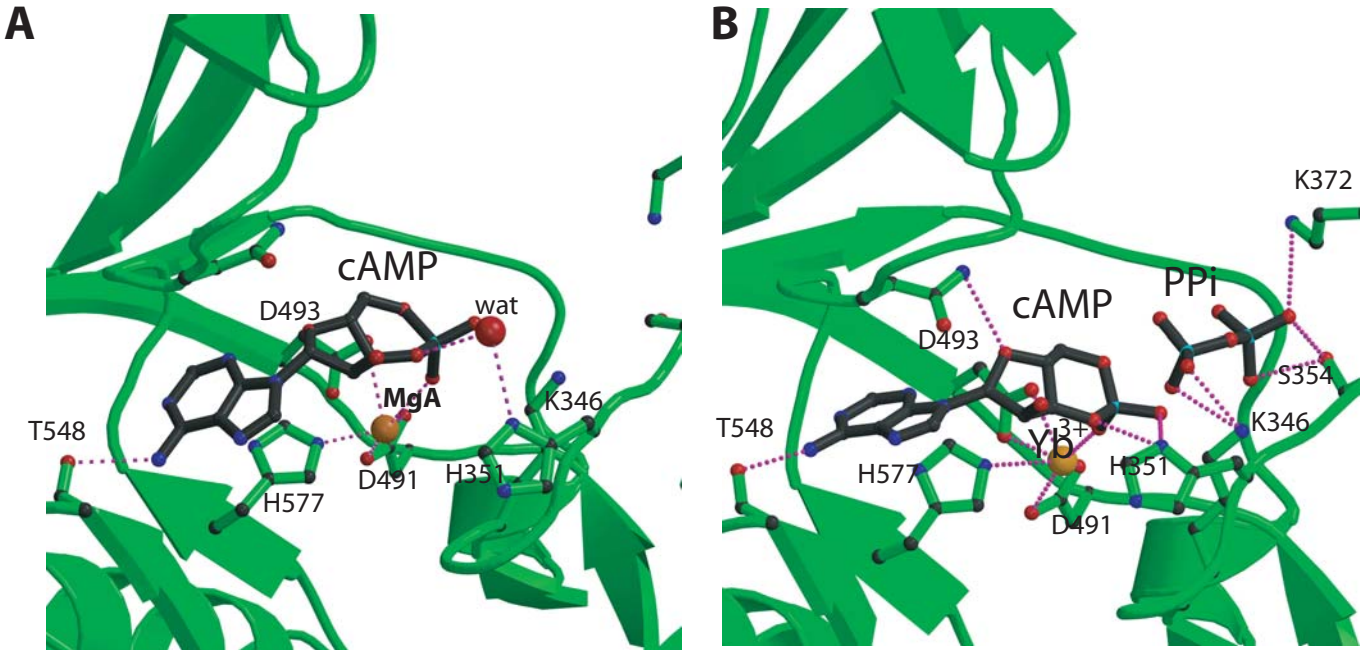

The comparison of active sites between EF-CaM (A) and EF-ACD-CaM (B) in complex with the reaction products, cyclic AMP (cAMP) and pyrophosphate (PPi). Oxygen, nitrogen, carbon and metal atoms are colored red, blue, black and orange, respectively. Backbone of EF proteins and reaction products are colored green and black, respectively. Hydrogen bonds are shown in magenta.

Supplemental figure 9

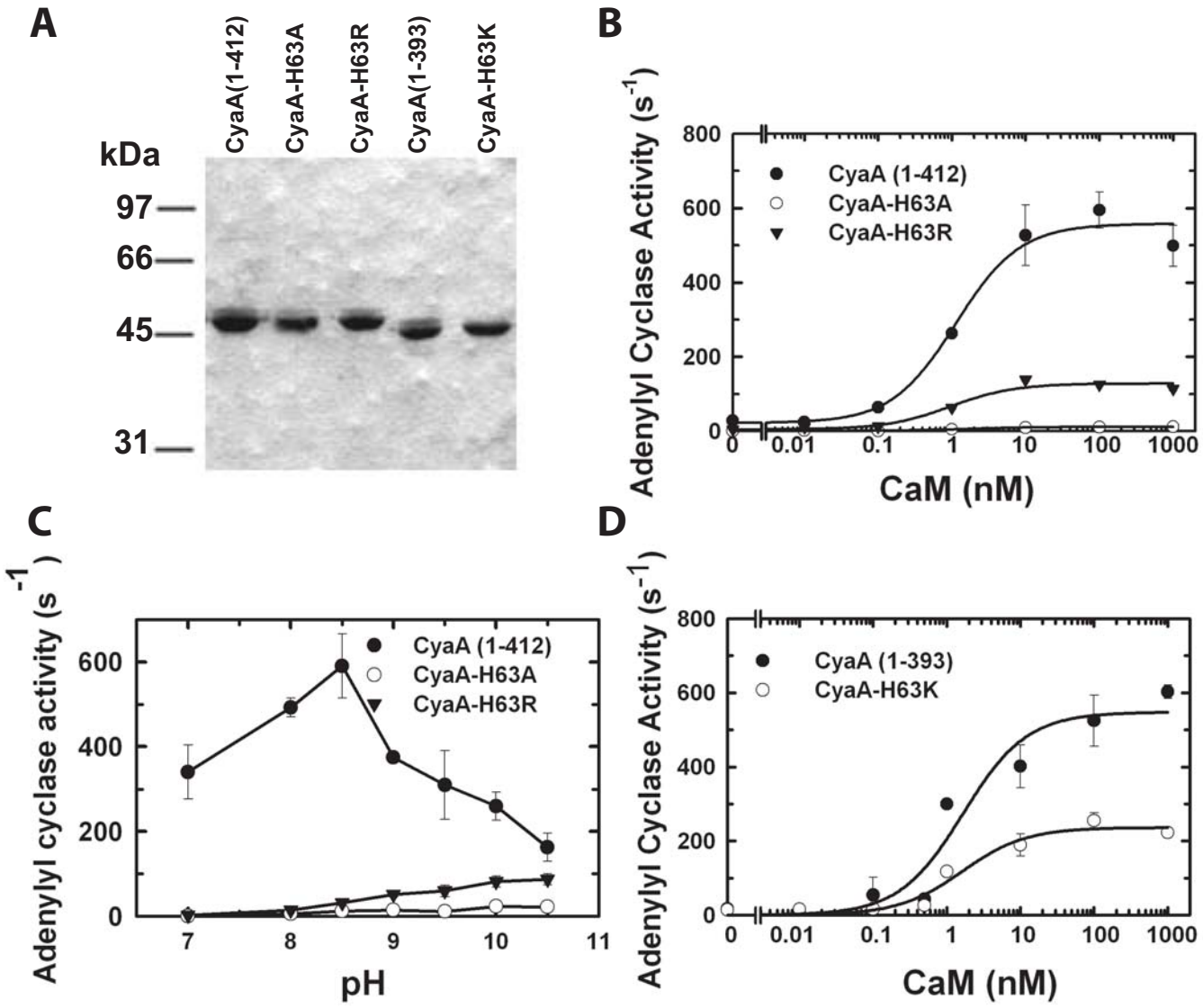

Effects of pH on the enzymatic activity of CyaA-ACD and its H63 mutants. (A) Coomassie blue staining of purified CyaA (1-412), H63A, H63R and CyaA (1-393) and H63K on SDS-PAGE (2 μg each). (B) Activation of CyaA (1-412), H63A, H63R by CaM. CyaA (1-412)(0.50 nM), H63A (5.0 nM) and H63R (5.0 nM) were assayed in the presence of the indicated CaM concentrations at pH 7.2. (C) Adenylyl cyclase activity of CyaA (1-412), H63A and H63R at the indicated pH. Adenylyl cyclase activity was measured using 10 mM ATP, 10 mM $MgCl_2$, 1.2 μM free $CaCl_2$, 1 μM CaM, and 0.5 mM BAPTA. (D) Acitvation of CyaA (1-393) and CyaA (1-393) H63K by CaM. CyaA (1-393) (0.50 nM) and H63K (0.8 nM) were assayed in the presence of the indicated CaM concentrations at pH 7.2. The reason to use CyaA (1-393) H63K mutant is due to the difficulty to obtain the stable CyaA (1-412) H63K protein.

Supplemental figure 10

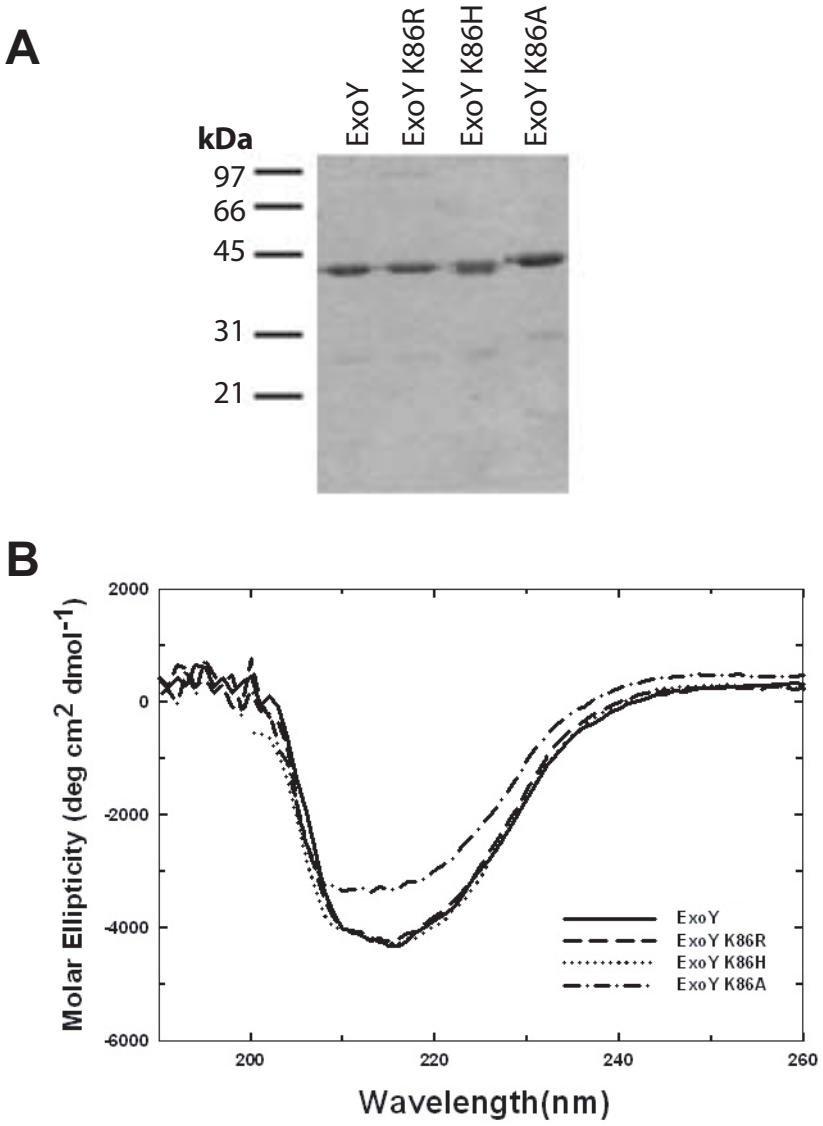

Biochemical studies of ExoY and its mutants. (A) Coomassie blue staining of purified ExoY and its mutants K86A, K86R, and K86H on SDS-PAGE (2 μg each). (B) Circular dichroism spectra of ExoY and its mutants. The measurements were taken using 1 μg/ml ExoY proteins following the experimental setup as described in supplemental figure 6.

Table 1S Additional refinement statistics of EF-CaM complexes

Crystal name	EF-CaM-Ca^{2+} (1μM)	EF-CaM-Ca^{2+} (1 mM)	EF-CaM-Ca^{2+} (10 mM)	EF-CaM-3'dATP	EF-CaM-cAMP	EF-Δ64-CaM	EF-CaM-PPi
independent reflections/ refined parameters*	0.69 (118,338 /171,408)	0.75 (12,913 /171,432)	0.77 (12,758 /17,1456)	0.67 (11,643 /172,200)	0.70 (12,066 /171,984)	0.71 (11,990 /171,432)	0.57 (9,746 /171,648)
$Rms_{dihedral}$(°)	22.8	22.5	22.3	23.2	22.7	22.8	22.8
$Rms_{improper}$(°)	1.08	1.36	1.15	1.06	1.01	0.94	1.06
Ramachandran plot (%)							
favorable	65.3	72.2	69.7	67.0	69.4	65.5	62.6
additional	34.7	27.8	30.3	33.0	30.6	34.5	33.4
generous	0	0	0	0	0	0	4.1
disallowed	0	0	0	0	0	0	0
G-factor	-0.1	0	0	-0.1	-0.1	-0.1	-0.1
No. of cis-peptide bond	0	0	0	0	0	0	0

* Non-crystallographic symmetry restraints are applied in six EF-CaM molecules in the same asymmetric unit during the refinement to improve the ratio of independent reflections/refined parameters.

Table 2S
Binding free energies and their electrostatic and van der Waals components from 2 ns molecular dynamics trajectories of EF-CaM, EF-ACD-CaM, and ATP·2Mg in aqueous solution.

Simulated System[a]	His351[b]	Energy (kcal/mol)			
		<ES>	<vdW>	ΔG[c]	$\Delta\Delta G_{bind}$[d]
ATP·2Mg in water		-50.8	-17.96	-35.4	
EF-CaM(A)	HIP	-25.5	-39.27	-34.8	0.7
EF-CaM(B)	HIP	-49.6	-36.3	-45.1	-9.7
EF-CaM(C)	HIP	-45.7	-35.87	-43.0	-7.5
EF-CaM(D)	HID	-26.0	-39.11	-34.9	0.5
EF-CaM(E)	HID	-61.0	-31.62	-48.2	-12.8
EF-CaM(F)	HID	-42.6	-35.22	-41.0	-5.6
average					-5.7
EF-ACD-CaM(A)	HID	-39.5	-37.18	-40.6	-5.1
EF-ACD-CaM(B)	HID	-51.9	-32.45	-44.1	-8.7
EF-ACD-CaM(B)	HIP	-46.1	-32.35	-41.1	-5.7
EF-ACD-CaM(C)	HID	-37.1	-37.27	-39.4	-4.0
EF-ACD-CaM(C)	HIP	-42.1	-36.99	-41.7	-6.3
average					-6.0

[a] pdb codes 1XFV for EF-CaM and 1K90 for EF-ACD-CaM were used. The specific EF-CaM and EF-ACD-CaM chains used as a starting point of the simulation are given in parenthesis.

[b] HIP denotes histidine with hydrogens bonded to both N_ε and N_δ (charge +1), HID denotes histidine with hydrogen bonded to Nd (charge 0). Total charged aminoacid residues: EF-CaM: ARG329 LYS333 LYS340 LYS346 HIP351/HID351 LYS353 ASP356 LYS372 LYS373 GLU381 LYS382 GLU386 LYS388 LYS389 GLU393 HID394/HIP394 GLU397 LYS479 ASP491 ASP493 ARG540 ASP543 LYS546 LYS554 ASP573 GLU580 ASP582 GLU585 GLU588 ASP590 GLU592, EF-ACD-CaM: ARG329 LYS333 LYS340 LYS346 HIP351 LYS353 ASP356 LYS372 LYS373 GLU381 LYS382 GLU386 LYS388 LYS389 GLU393 HIP394 GLU397/GL0397 LYS479 ASP491 ASP493 ARG540 ASP543 LYS546 LYS554 ASP573 GLU580 ASP582 GLU585 GLU588 ASP590 GLU592

[c] $\Delta G = 0.5 <ES> + 0.56*<vdW>$, where <ES> and <vdW> are, respectively, the electrostatic and van der Waals interaction energy components averaged over the simulated trajectory.

[d] $\Delta\Delta G_{bind} = \Delta G_{protein} - \Delta G_{water}$ is binding free energy.